105 anos 1916 • 2021

An Acad Bras Cienc (2021) 93(Suppl. 4): e20210535 DOI 10.1590/0001-3765202120210535
Anais da Academia Brasileira de Ciências | *Annals of the Brazilian Academy of Sciences*
Printed ISSN 0001-3765 I Online ISSN 1678-2690
www.scielo.br/aabc | www.fb.com/aabcjournal

GEOSCIENCES

Crystallization conditions of two adjacent epidote + diopside-bearing granitic stocks, northeastern Brazil

RENAN SIQUEIRA, ALCIDES N. SIAL & VALDEREZ PINTO FERREIRA

Abstract: The Tamboril and Olho d'Água granitic stocks are part of the abundant calc-alkalic magmatic epidote-bearing granitic rocks in the Cachoeirinha–Salgueiro Terrane (CST) in the Transversal Zone Domain, northeastern Brazil. The equigranular Olho d'Água stock is composed of medium-grained clinopyroxene-amphibole–biotite tonalite; the porphyritic Tamboril stock is medium- to coarse-grained amphibole biotite ± clinopyroxene granodiorite. Abundances of clinopyroxene and epidote vary inversely in both stocks. Amphibole–rich clots are regarded as fragments from the source region captured by granodioritic/tonalitic magma during its ascent. Epidote composition in the Olho d'Água stock ($Ps_{18–26}$) and in Tamboril stock (Ps_{17-20}) is consistent with crystallization under oxygen fugacity between QFM and HM buffers. In the Olho d'Água stock, calculated values of pressure range from 5.1 to 6.6 kbar and in the Tamboril stock from 6.2 to 7.0 kbar. Solidification temperatures estimated from plagioclase-hornblende pairs in the Olho D´Água stock range from 637 to 679 °C and for Tamboril from 587 to 641 °C. Zr-saturation temperature estimates are 788 to 819 °C (Olho d'Água) and 807 to 829 °C (Tamboril). Altogether our data suggest that the studied stocks crystallized from two distinct magmatic pulses formed from fractional melting of a single amphibolitic source. These two magma pulses underwent subsequent crystallization, in a convective magmatic chamber, at rather high pressure.

Key words: calc–alkalic granites, magmatic epidote, clinopyroxene, thermobarometry, oxygen fugacity.

INTRODUCTION

Neoproterozoic calc-alkalic and high-K calc-alkalic granodioritic to tonalitic plutons intruded Neoproterozoic low-grade metasedimentary rocks of the Cachoeirinha–Salgueiro (CST) and Alto Pajeú (APT) terranes in northeastern Brazil. These plutons are made up of medium–grained equi- to inequigranular rocks that commonly contain magmatic epidote (mEp) crystals up to 2 mm long. They exhibit a texture, informally described as *"toad leather"*, which is characteristic of granites regionally known as of the Conceição type (Sial 1984). In some of these plutons, samples with lower-abundance of mEp have higher-abundance of clinopyroxene (e.g. Pedra Branca, Tamboril, Angico Torto, Minador plutons; Sial et al. 1999, and also the Coronel João Sá pluton in the Macururé Domain (Long et al. 2005). Extensive reviews on petrography and geochemistry of these plutons are found in Sial et al. (1999, 2008) and Brasilino et al. 2011.

This study concerns two such plutons: Tamboril and Olho d'Água (Fig. 1). Although a single NE—SW trending elongate "Tamboril" pluton was initially mapped, we have distinguished two adjacent stocks, renamed as Tamboril and Olho d'Água, whose P-T conditions

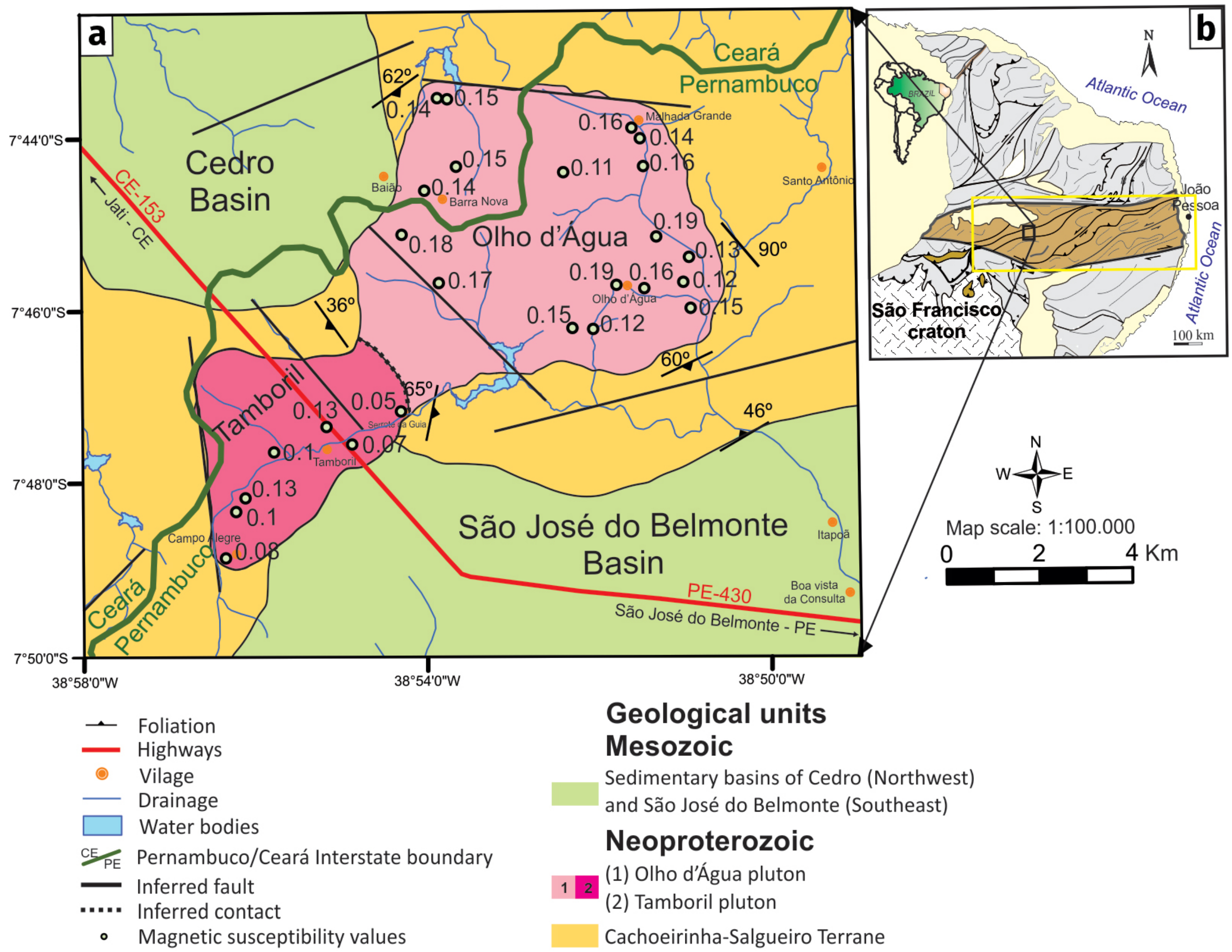

Figure 1. (a) Simplified geological map of the study area and the magnetic susceptibility values of Tamboril and Olho d'Água stocks. (b) Location of the Transversal Zone within the Borborema Province, Northeast of Brazil. Modified from Siqueira et al. (2018).

of crystallization differ. Both plutons bear magmatic epidote (mEp) but they also carry clinopyroxene, which is normally absent. The contact zone between the two "facies" is severely weathered, and only after an examination of the mineral chemistries and thermobarometric estimates did it become clear that they are actually two adjacent stocks.

This study aims to: (a) understand the conditions of coexistence of magmatic epidote with clinopyroxene, (b) characterize the mineral chemistry of these mEp–bearing granitoids; (c) estimate crystallization temperatures and pressures, which differ; (d) understand the geologic environment of formation.

MAGMATIC EPIDOTE AND CLINOPYROXENE IN GRANITIC PLUTONS IN THE CST

In the Cachoeirinha–Salgueiro Terrane, only the Pedra Branca and Angito Torto plutons, 100 km apart from one another, are so far known to contain both mEp and cpx. In the Pedra Branca pluton, abundant calcic clinopyroxene crystals up to 3 cm long commonly show rims partially transformed into hornblende, suggesting disequilibrium with the host melt (Sial et al. 1998). In minor epidote, pistacite contents [Ps = molar $100*Fe^{3+}/(Fe^{3+}+Al^{3+})$] vary between Ps_{19} and Ps_{24}. Not all of the values of pistacite point to a magmatic origin of this epidote (Sial 1990).

Similarly, in the Angico Torto pluton, cpx occurs as crystals up to 1 cm long, accompanied by four different types of less-abundant mEp, two of them of probable magmatic origin, displaying chemical zonation and allanite–rich cores (Sial 1990).

In the unfoliated Coronel João Sá batholith, intrusive into the Sergipano Belt, Macururé Domain, magmatic epidote coexists with strongly resorbed clinopyroxene. In this batholith, which comprises two adjacent plutons, clinopyroxene (augite–diopside) is present in the northern pluton and in the western portion of the southern pluton. Partially resorbed clinopyroxene laths, up to 1.5 cm long, are replaced by hornblende, biotite, or epidote, leaving disaggregated clinopyroxene (cpx) grains that are in optical continuity (Long et al. 2005). Textural characteristics of epidote indicate magmatic origin. Below, we compare the commonalities of the Pedra Branca, Angico Torto, and Coronel João Sá bodies with Tamboril and Olho D´Água, the subject of this paper.

PREVIOUS WORKS

The Tamboril and Olho D´Água stocks, exposed for over than 70 km², were intruded into low- to intermediate- grade metasedimentary rocks of the Santana dos Garrotes Formation (Cachoeirinha Group), which consists predominantly of metapelite, metapsammite, metaconglomerate, and to a much lesser extent, metavolcanic rocks, marble, and banded iron formation. TIMS U–Pb zircon ages in the 660–620 Ma interval were determined in metavolcanic rocks of this Group (Van Schmus et al. 2011).

According to Siqueira et al. (2018), the Olho d'Água stock is composed of medium–grained, equigranular clinopyroxene–biotite tonalite containing amphibole, magmatic epidote, and titanite. The Tamboril stock is a coarse- grained porphyritic granodiorite, with quartz plagioclase megacrysts, K-feldspar, biotite, amphibole, magmatic epidote, ± clinopyroxene, and titanite. The former stock is faulted in its western contact and the latter in its northern contact, and they were emplaced along a regional SW–NE trending fracture (Fig. 1). Mafic syn–plutonic dikes are observed only in the Olho d´Água stock. In the Tamboril stock, up to 50 cm wide pegmatitic dikes record multiple injections of felsic magma and in some of than comb structure are present.

Enclaves

The Olho d´Água stock exhibits abundant dioritic enclaves up to one meter long. These enclaves show crenulated margins in contact with tonalitic to granodioritic host rock, indicating that both lithologies, of different magmatic viscosities, had been in a magmatic state. In some of these mafic enclaves, ellipsoidal K-feldspar crystals seem to have been captured from the tonalite magma, suggesting a degree of mixing.

Sial et al. (1998) described two types of amphibole–rich clots (ARCs) in mEp–bearing calc–alkalic plutons intruded into the Cachoeirinha–Salgueiro Terrane. One type consists of dark green calcic amphibole aggregates interpretated to have fractionated from the host magma; the other type, consisting of amphibole aggregates up to 15 cm long, exhibits fine-grained texture (Sial et al. 1998). The second type, with crystals up to 5 cm long, is mainly composed of actinolite amphibole with magnesio-hornblende margins, regarded as source fragments captured by granodioritic/tonalitic magmas (Sial et al. 2008, Sial & Ferreira 2015). Typically a biotite + amphibole layer armors the second type, thus to have inhibited further interaction with the host magma. Both ARC types are present in the Olho d'Água and Tamboril plutons. One of them is angular in shape, suggesting extraction from the source in a solid state (Fig. 2c); the other type is armored by biotite crystallized from the host magma (Fig. 2d).

Olho D´Água tonalite and Tamboril granodiorite

The studied stocks are high–K calc–alkalic, metaluminous, Mg-type Cordilleran tonalitic to granodioritic rocks, but their data points plot in discrete fields in the same diagrams, exhibiting two independent trends (Siqueira et al. 2018). Both tonalite-granodiorite and enclaves carry clinopyroxene, in both plutons clinopyroxene in host rock is unrelated to clinopyroxene in the enclaves (Siqueira et al. 2018). In the host tonalite, elongate clinopyroxene up to 2 cm long occupies 5 to 10% of the rock volume (Fig. 2e). In the diorite enclaves, elongate poikilitic crystals up to 4 cm long occupy up to 25% of the volume. Abundant small inclusions are comprised of anhedral amphibole, biotite, and titanite (Fig. 2f). Uralitized clinopyroxene in the

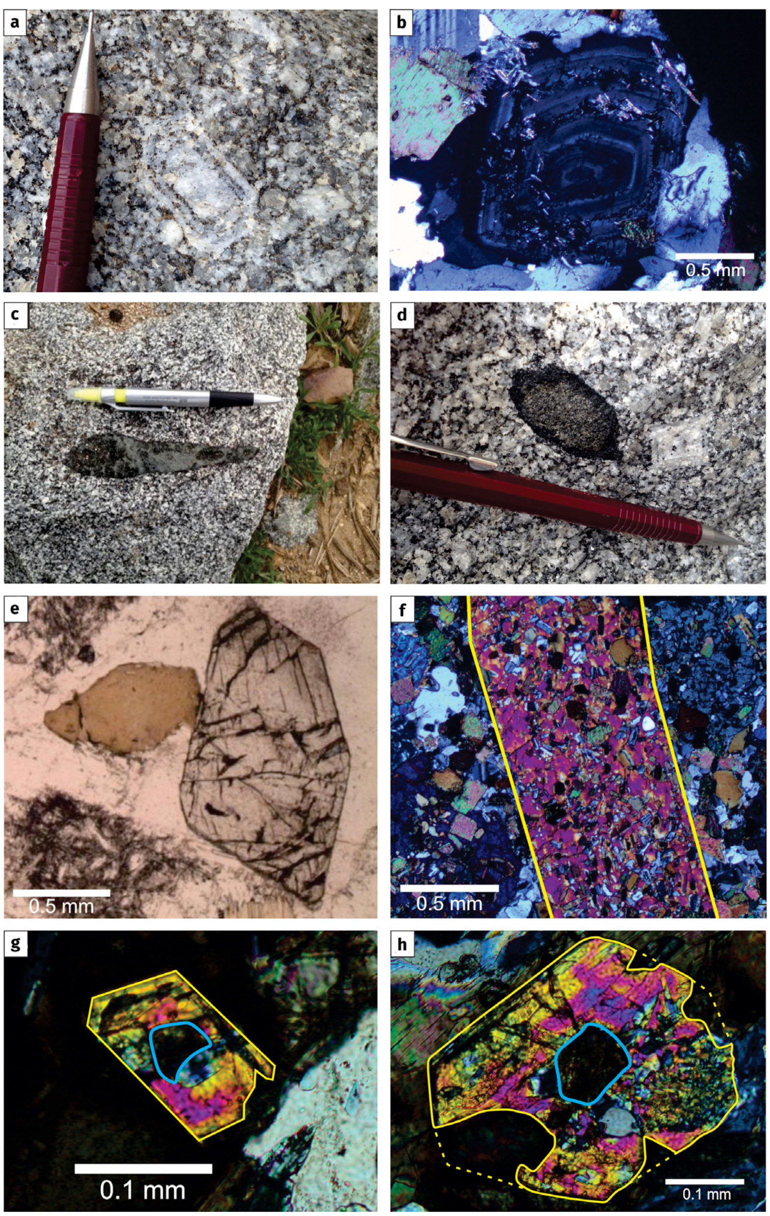

Figure 2. Geological and petrographic aspects of Tamboril and Olho d'Água plutons: (a) biotite rows at euhedric plagioclase; (b) Plagioclase megacrysts with oscillatory zoning and biotite rows; (c) angular–shaped of calcic amphibole rich clot; (d) amphibole rich clot armored by biotite; (e) euhedral clinopyroxene without inclusions; (f) Clinopyroxene with poikilitic texture; (g–h) euhedral magmatic epidote (mEp) with allanite nucleus and compositional zoning.

host tonalites are observed, probably due to subsolidus hydrothermal alteration.

Plagioclase, up to 4 cm long, in the Tamboril pluton exhibits polysynthetic twinning, synneusis, myrmekitic intergrowth lamellae and wavy extinction, all of which resulted from solid–state deformation. Plagioclase megacrysts also display oscillatory zoning in, and biotite rows (double concentric rows in some cases; Fig. 2a), attest that the host magma had experienced multiple pulses of magma injection, possibly associated with convection.

Sial et al. (2008) described four types of magmatic epidote textural relationships: type 1 mEp is embayed or in vermicular contact with unaltered plagioclase; type 2 mEp is rimmed by biotite and exhibits zoned allanite cores; type 3 mEp encloses patches of hornblende and in type 4, mEp is partially enclosed by biotite in the interstices of K-feldspar aggregates. Siqueira et al. (2018) identified only the type 2 mEp in both the Olho d'Água and Tamboril stocks, besides anhedral to subhedral, very elongated crystals of dubious origin in the core of plagioclase megacrysts, and epidote as product of plagioclase saussuritization.

For both plutons, all of these characteristics — presence of amphibole rich clots (ARC), magmatic epidote, euhedral titanite, clinopyroxene, calcic amphibole, and calc-alkalic and metaluminous whole-rock chemistry — have been recognized as diagnostic indicators of I-type granitoides (Siqueira et al. 2018).

ANALYTICAL METHODS

The mineral chemical analyses were carried out at the Institute of Geosciences, University of Brasília, Brazil. Thin sections were covered by a carbon film in a vacuum chamber and analyzed in a JEOL model JXA–8230 electron microprobe, with one EDS and five WDS spectrometers. For major element analysis an acceleration voltage of 15 kV, current of 10 nA, and a diameter of 1 μm of the electronic beam were used for analyzing feldspar, amphibole, biotite, epidote, titanite, and clinopyroxene. Mineral standards were: Na_2O (albite gaspox), MgO (forsterite), F (topaz), Al_2O_3 (microcline), SiO_2 (microcline), TiO_2 ($MnTiO_3$), Cr_2O_3 (Cr_2O_3), MnO ($MnTiO_3$), K_2O (microcline), CaO (andradite gaspox), NiO (NiO), FeO (andradite gaspox), V_2O_3 (vanadinite), Cl (vanadinite).

Clinopyroxene structural formula was calculated based on 6 oxygens and 4 cations, as well as the percentages of wollastonite (Wo = $Ca_2Si_2O_6$), enstatite (En = $Mg_2Si_2O_6$) and ferrosilite (Fs = $Fe_2Si_2O_6$). Plagioclase compositions were calculated based on 5 cations and 8 oxygens, biotite on 20 cations and 24 oxygens, epidote on 8 cations and 12.5 oxygens, titanite on 12 cations and 20 oxygens, and amphibole on 13 cations and 23 oxygens. The Tindle & Webb (1990) procedure was used to calculate Li_2O and H_2O of biotite and the Tindle & Webb (1994) methods to partition Fe^{2+} and Fe^{3+}, and calculate H_2O contents of amphibole.

MINERAL CHEMISTRY

Feldspar

Tamboril plagioclase is mostly An_{18-34} (oligoclase–andesine), whereas Olho d'Água plagioclase varies from An_4 to An_{42} (albite–andesine) (Fig. 3) (Table I, Supplementary material – Table SI). A profile (core–rim) performed on a plagioclase phenocryst of the Tamboril pluton demonstrates a smooth reverse zoning with a nucleus slightly enriched in Na and depleted in Ca.

Amphibole

Amphibole is calcic (Leake et al. 1997) (Table II, Table SII). Amphibole in the Tamboril pluton and its dioritic enclaves is mostly ferro-edenite,

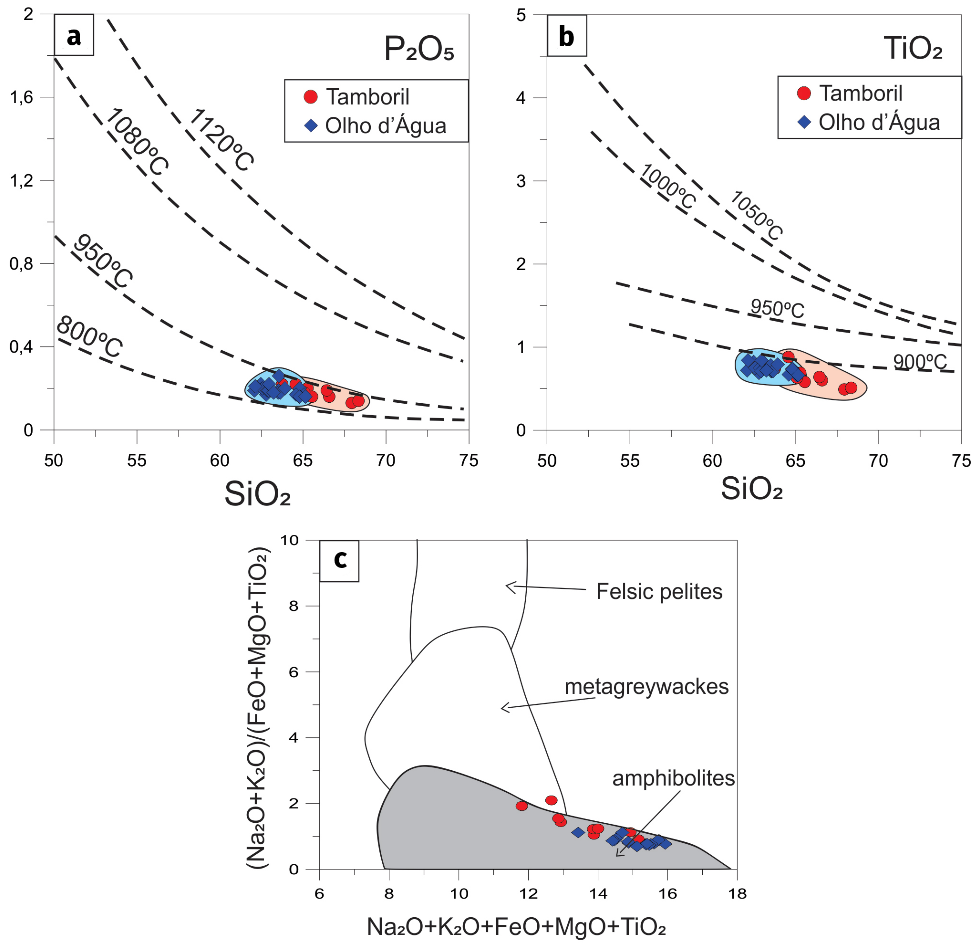

Figure 3. **Isotherms in (a) and (b) are respectively from Green and Watson (1982) and Green and Pearson (1986), with silica versus oxides (in wt.%) diagrams for the Tamboril and Olho d'Água plutns. (c) Douce (1999) experimental diagram.**

whereas Olho d'Água amphibole is edenite to Fe-pargasite (Fig. 4a), althougth slightly more magnesian than Tamboril amphibole, that is similar to amphiboles in plutons elsewhere in the Cachoeirinha–Salgueiro Terrane (e.g) Brasilino et al. (2011). Mg/(Mg+Fe) cationic ratios in edenite (0.45–0.70) are in the range proposed by Mason (1985) for amphibole from alkali-calcic granitoids; Fe/(Fe+Mg) ratios correspond to moderately high oxygen fugacity during crystallization of this phase. Alternatively, the availability of Fe can have also played some influence on the Fe/(Fe+Mg) ratio. A positive correlation between Al^{IV} and Al^{T} in amphibole (Fig. 4b) is similar to that reported by Hammarstrom & Zen (1986), which reflects perhaps crystallization of amphibole during ascent of magma. In Olho d'Água stock, amphibole has alumina saturation index (ASI = $Al_2O_3/(CaO + Na_2O + K_2O)$ molar) about 0.62-0.94 and in Tamboril stock ASI is around 0.65-0.79.

Biotite

In the Al^{T} *vs.* Mg atoms per formula unit (apfu) diagram, the biotite compositions (Table III, Table SIII) from the Tamboril stock plot within the field for biotite of the calc–alkalic series of igneous rocks (Fig. 5a), while biotite composition from the Olho D´Água stock straddles from the sub-alkalic to the calc-alkalic fields. The Al^{IV} vs Fe# diagram (Deer et al. 1992) (Fig. 5b) shows that trends for the two stocks are distinct, with biotite from the Olho D´ Água stock showing a larger Al^{IV} variation than of biotite from the other stock, both a with limited Fe# variation. In the MgO *vs.*

Table I. **Microprobe analyses of plagioclase from Tamboril (TAM) and Olho d'Água (OA) plutons.**

Sample	**BELRS-2A**	**BELRS-2A**	**BELRS-2A**	**BELRS-2A**	**BELRS-2A**	**BELRS-2A**	**BELRS-13A**	**BELRS-13A**	**BELRS-20A**	**BELRS-20A**	**BELRS-31**	**BELRS-31**
Position	Center	Rim	Center	Rim	Center	Rim	Center	Rim	Center	Rim	Center	Rim
Pluton	TAM	TAM	TAM	TAM	TAM	TAM	OA	OA	OA	OA	OA	OA
SiO_2	59.32	62.66	60.82	62.23	62.76	63.12	57.50	60.52	61.10	66.48	58.01	62.62
TiO_2	<dl	<dl	0.06	<dl	0.04	<dl	<dl	0.05	0.07	0.07	<dl	<dl
Al_2O_3	25.93	23.47	25.31	23.48	24.22	23.17	26.60	23.93	25.14	22.64	26.17	23.80
FeO	<dl	0.09	<dl	<dl	<dl	0.03	<dl	0.15	0.07	0.13	0.13	0.10
MnO	0.04	<dl	0.04	0.03	<dl	0.13	<dl	0.02	0.13	<dl	0.06	<dl
MgO	<dl	<dl	<dl	0.01	<dl	0.01	0.02	<dl	<dl	0.02	<dl	0.01
CaO	7.03	4.87	6.41	4.96	5.41	4.33	8.42	5.13	7.37	4.06	7.95	4.77
BaO	0.08	<dl	<dl	<dl	0.08	0.10	<dl	0.03	<dl	<dl	<dl	0.06
Na_2O	7.79	9.17	8.17	8.95	8.67	9.47	6.89	8.94	7.40	9.27	7.08	9.08
K_2O	0.13	0.11	0.16	0.19	0.09	0.14	0.09	0.05	0.18	0.13	0.26	0.19
Total	100.32	100.36	100.98	99.84	101.27	100.51	99.52	98.82	101.44	102.81	99.65	100.63
	Cation proportions are based on 8 oxygens											
Si	2.631	2.760	2.676	2.757	2.749	2.773	2.581	2.706	2.694	2.867	2.598	2.752
Ti	<dl	<dl	0.002	<dl	0.001	<dl	<dl	0.002	0.002	0.002	<dl	<dl
Al	1.355	1.218	1.312	1.226	1.250	1.200	1.408	1.261	1.306	1.151	1.382	1.233
Fe	<dl	0.003	<dl	<dl	<dl	0.001	<dl	0.006	0.003	0.005	0.005	0.004
Mn	0.001	<dl	0.001	0.001	<dl	0.005	<dl	0.001	0.005	<dl	0.002	<dl
Mg	<dl	<dl	<dl	0.001	<dl	0.001	0.002	<dl	<dl	0.001	<dl	0.001
Ca	0.334	0.230	0.302	0.235	0.254	0.204	0.405	0.246	0.348	0.188	0.382	0.225
Ba	0.001	<dl	<dl	<dl	0.001	0.002	<dl	0.001	<dl	<dl	<dl	0.001
Na	0.670	0.783	0.697	0.769	0.736	0.807	0.599	0.775	0.633	0.775	0.615	0.773
K	0.007	0.006	0.009	0.011	0.005	0.008	0.005	0.003	0.010	0.007	0.015	0.011
Sum	5,000	5,000	5,000	5,000	4,997	5,000	5,000	4,999	5,000	4,996	4,998	4,999
Mol.% An	33.048	22.548	29.957	23.203	25.511	19.997	40.121	24.031	35.134	19.339	37.734	22.260
Mol.% Ab	66.252	76.862	69.142	75.761	73.989	79.222	59.396	75.713	63.873	79.902	60.802	76.662
Mol.% Or	0.700	0.590	0.902	1.036	0.500	0.781	0.482	0.256	0.994	0.760	1.464	1.078

<dl: below detection limits.

Al_2O_3 diagram, the biotite compositions of both plutons plot in the field of calc–alkalic series of igneous rocks (Fig. 5c), compatible with the calc-alkalic nature of host rock (Siqueira et al. 2018). The average value of FeO/MgO (1.76) for biotite in these stocks is similar to ratios reported by Brasilino et al. (2011) from other calc–alkalic granites from the Cachoeirinha-Salgueiro Terrane. The alumina saturation index from the biotite of these stocks between 1.38–1.86 reflects low alumina activity in the crystallizing magma (Zen 1988). Under these conditions, it is common to form Ca-rich and low-Al mineral phases, such as hornblende and epidote.

Table II. **Microprobe analyses of amphibole from Tamboril (TAM) and Olho d'Água (OA) plutons. Tindle & Webb (1994) methods calculated to Fe partition (Fe^{2+} – Fe^{3+}) and H_2O contents.**

Sample	BELRS-2A	BELRS-2A	BELRS-2A	BELRS-2A	BELRS-2A	BELRS-2A	BELRS-13A	BELRS-13A	BELRS-13A	BELRS-13A	BELRS-19B	BELRS-19A	BELRS-19A
Position	Center	Rim	Center	Rim	Center	Rim	Center	Rim	Center	Rim	Center	Center	Rim
Pluton	TAM	TAM	TAM	TAM	TAM	TAM	OA	OA	OA	OA	OA	OA	OA
SiO_2	43.502	43.674	43.304	43.648	43.751	43.73	48.458	46.128	46.25	42.568	45.421	46.424	41.921
TiO_2	1.313	0.682	1.221	0.87	1.066	1.325	1.24	1.007	1.023	2.158	1.595	1.612	1.63
Al_2O_3	10.902	10.679	10.544	10.899	10.787	11.04	7.477	9.707	8.779	11.397	8.706	7.653	11.097
FeO	17.358	16.816	17.013	17.117	18.477	17.443	15.912	14.625	16.993	17.76	14.136	14.12	16.325
MgO	8.393	8.435	8.347	8.347	8.494	8.342	11.918	11.802	10.25	8.602	11.106	11.234	11.143
MnO	0.229	0.381	0.36	0.354	0.224	0.338	0.301	0.096	0.339	0.243	0.493	0.4	0.223
CaO	11.548	11.425	11.461	11.547	11.39	11.401	11.533	11.517	11.82	11.326	11.406	11.244	6.167
Na_2O	1.491	1.393	1.563	1.614	1.557	1.543	1.365	1.672	1.251	1.56	1.507	1.374	0.594
K2O	1.323	1.307	1.274	1.33	1.373	1.336	0.525	0.744	0.962	1.143	0.902	0.604	5.032
F	0.157	0.184	0.15	0.285	0.161	0.135	0.163	0.256	0.16	0.218	0.028	0.045	0.146
Cl	0.014	<dl	0.014	<dl	0.002	0.006	<dl	0.007	0.022	0.005	0.013	0.012	0.009
Sum	96.23	96.10	95.25	96.01	97.28	96.64	98.89	97.56	97.85	96.98	95.31	94.72	94.29
	Cation proportions are based on 23 oxygens.												
T-sites													
Si	6.650	6.743	6.690	6.696	6.628	6.650	7.033	6.788	6.881	6.457	6.863	7.025	6.614
Al^{iv}	1.350	1.257	1.310	1.304	1.372	1.350	0.967	1.212	1.119	1.543	1.137	0.975	1.386
Sum	8.000	8.000	8.000	8.000	8.000	8.000	8.000	8.000	8.000	8.000	8.000	8.000	8.000
M1.2.3 sites													
Al^{vi}	0.615	0.687	0.610	0.667	0.555	0.630	0.312	0.473	0.421	0.496	0.414	0.390	0.678
Ti	0.151	0.079	0.142	0.100	0.121	0.152	0.135	0.111	0.114	0.246	0.181	0.183	0.193
Fe^{3+}	0.096	0.100	0.066	0.064	0.226	0.120	0.329	0.298	0.228	0.250	0.161	0.161	0.311
Mg	1.912	1.941	1.922	1.908	1.918	1.891	2.578	2.588	2.273	1.945	2.501	2.533	2.620
Mn	0.030	0.050	0.047	0.046	0.029	0.044	0.037	0.012	0.043	0.031	0.063	0.051	0.030
Fe^{2+}	2.123	2.071	2.132	2.132	2.115	2.099	1.602	1.502	1.886	2.003	1.625	1.626	1.789
Ca	0.073	0.072	0.081	0.082	0.036	0.066	0.006	0.015	0.035	0.029	0.055	0.055	0.000
Sum	5.000	5.000	5.000	5.000	5.000	5.000	5.000	5.000	5.000	5.000	5.000	5.000	5.000
M4 site													
Fe	<dl	<dl	<dl	<dl	<dl	<dl	<dl	<dl	<dl	<dl	<dl	<dl	0.676
Ca	1.819	1.818	1.816	1.816	1.813	1.792	1.787	1.801	1.849	1.812	1.792	1.769	1.043
Na	0.181	0.182	0.184	0.184	0.187	0.208	0.213	0.199	0.151	0.188	0.208	0.231	0.282
Sum	2.000	2.000	2.000	2.000	2.000	2.000	2.000	2.000	2.000	2.000	2.000	2.000	2.000
A site													
Ca	<dl	<dl	<dl	<dl	<dl	<dl	<dl	<dl	<dl	<dl	<dl	<dl	<dl
Na	0.261	0.235	0.284	0.296	0.270	0.247	0.171	0.278	0.210	0.271	0.234	0.172	-0.100
K	0.258	0.257	0.251	0.260	0.265	0.259	0.097	0.140	0.183	0.221	0.174	0.117	1.013
Sum A	0.519	0.493	0.535	0.556	0.536	0.506	0.268	0.417	0.392	0.492	0.408	0.288	0.913
OH site													
OH	1.920	1.910	1.923	1.862	1.922	1.933	1.925	1.878	1.919	1.894	1.983	1.975	1.925
F	0.076	0.090	0.073	0.138	0.078	0.065	0.075	0.120	0.076	0.105	0.013	0.022	0.072
Cl	0.004	<dl	<dl	<dl	<dl	0.002	<dl	0.002	0.006	0.001	0.003	0.003	0.002
Sum	2.000	2.000	2.000	2.000	2.000	2.000	2.000	2.000	2.000	2.000	2.000	2.000	2.000
Sum cations	15.519	15.493	15.535	15.556	15.536	15.506	15.268	15.417	15.392	15.492	15.408	15.288	15.913
Fe#	0.537	0.528	0.534	0.535	0.550	0.540	0.428	0.410	0.482	0.537	0.417	0.414	0.451
Mg/Fe^{2+}	0.901	0.937	0.901	0.895	0.907	0.901	1.609	1.723	1.205	0.971	1.539	1.558	1.063
Mg/Fe	0.862	0.894	0.874	0.869	0.819	0.852	1.335	1.438	1.075	0.863	1.400	1.418	1.216
$Mg/(Mg+Fe^{2+})$	0.382	0.388	0.384	0.382	0.384	0.378	0.516	0.518	0.455	0.389	0.500	0.507	0.524

<dl: below detection limits.

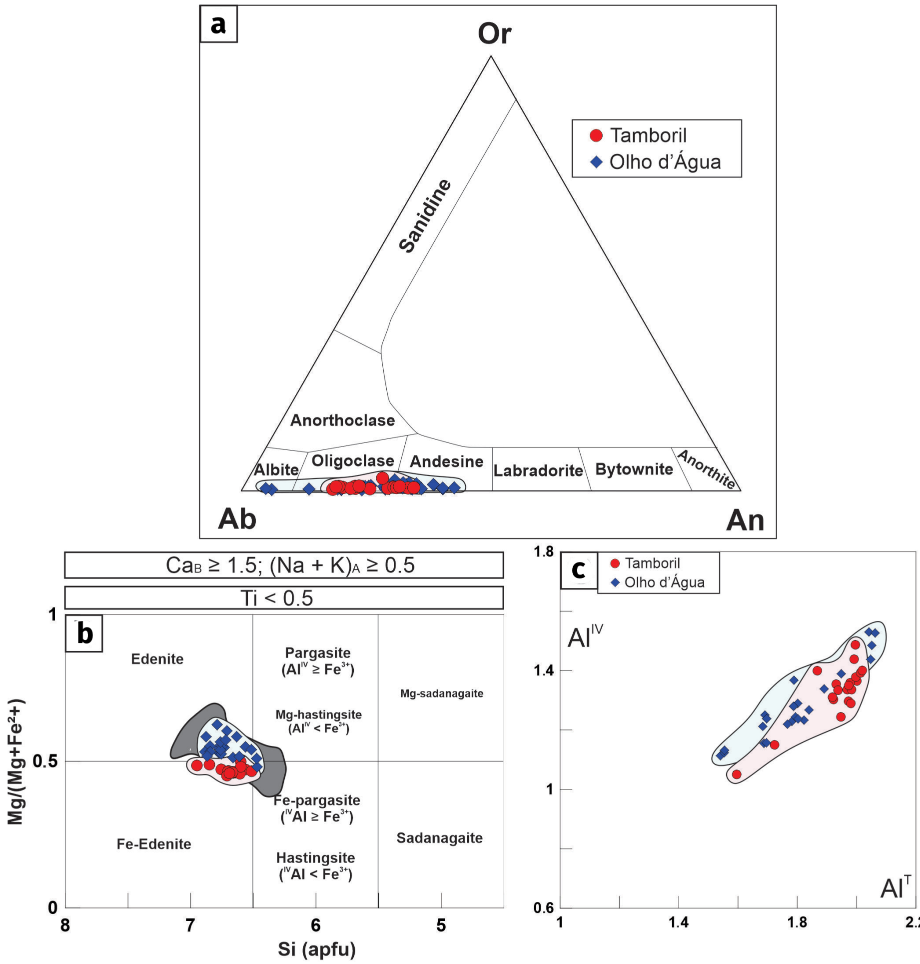

Figure 4. (a) Anorthite–Albite–Orthoclase ternary diagram (Deer et al. 1992) showing the compositions of feldspars from the Tamboril and Olho d´Água plutons; (b) Classification of amphiboles after Leake et al. (1997) compared with results obtained by Brasilino et al. (2011) (gray field); (c) Relationship between Al^{IV} and Al^{T} in the amphiboles of Tamboril and Olho d'Água plutons.

Epidote

Most epidote grains are zoned in which Fe^{+3} decreases from center to edge. Euhedral and sub-euhedral epidote present distinct molar pistacite, from Ps_{17-20}, avg. Ps_{18} (Tamboril) to Ps_{18-26}, avg. Ps_{21} (Olho d'Água) (Table IV, Table SIV).

Titanite

Titanite compositions (Table V, Table SV) in the Olho d'Água stock display positive correlation between Al and F (Fig. 5d), with Al contents in the 0.16 to 0.34 apfu range and fluorine in the 0 to 0.36 range. Based on Franz & Spear (1985), these chemical features argue that titanite crystallized at high pressure, a contention that finds further support in observations by Evans & Patrick (1987) and Tropper et al. (2002).

Clinopyroxene

The analyzed clinopyroxene grains (Table VI, Table SVI) from both plutons and their enclaves are generally rich in calcium and have low iron content (from 7.2 to 13.1% FeO), which makes their compositon to plot in the diopside field (Morimoto 1988) (Fig. 6). Clinopyroxene in host rock and diorite enclaves are similar, even though these lithologies are texturally different.

THERMOBAROMETRIC ESTIMATES

Temperature estimates using hornblende–plagioclase

Blundy & Holland (1990) proposed a thermometer (BH thermometer) based on amphibole–plagioclase relation, applied to temperatures

Table III. Microprobe analyses of biotite from Tamboril (TAM) and Olho d'Água (OA) plutons. Tindle & Webb (1990) approach was used to calculate Li_2O and H_2O contents.

Sample	**BELRS-10B**	**BELRS-10B**	**BELRS-10B**	**BELRS-10B**	**BELRS-10B**	**BELRS-19A**	**BELRS-19A**	**BELRS-27**	**BELRS-27**	**BELRS-32**	**BELRS-32**
Position	Center	Center	Rim	Center	Rim	Center	Rim	Center	Rim	Center	Rim
Pluton	TAM	TAM	TAM	TAM	TAM	OA	OA	OA	OA	OA	OA
SiO_2	36.80	36.66	36.55	35.53	36.25	36.72	37.00	36.07	36.59	36.37	36.54
TiO_2	1.60	1.87	1.22	0.90	1.20	2.34	2.31	3.29	2.72	2.92	2.39
Al_2O_3	16.10	16.00	15.95	15.76	15.99	15.38	15.60	15.32	15.63	15.20	14.75
FeO	23.16	22.54	23.99	23.77	22.33	16.36	16.57	16.95	16.31	18.87	18.94
MnO	0.26	0.26	0.16	0.39	0.17	0.18	0.16	0.10	0.16	0.33	0.23
MgO	9.00	9.03	9.43	9.94	9.59	10.56	10.96	10.79	11.48	9.98	10.65
CaO	0.01	0.04	<dl	0.03	0.04	0.02	0.01	0.04	0.02	0.07	0.08
Na_2O	0.04	0.07	0.09	0.05	0.08	0.06	0.05	0.05	0.07	0.03	0.08
K_2O	9.14	9.20	8.99	7.72	8.87	9.46	9.18	9.74	9.89	9.11	9.15
BaO	0.26	0.15	0.25	0.16	0.36	0.18	0.29	0.48	0.04	0.57	0.03
F	0.68	0.94	0.96	0.47	0.62	0.34	0.23	0.31	0.28	0.42	0.39
Cl	0.01	0.01	<dl	0.01	<dl	0.01	0.01	<dl	0.01	<dl	0.01
Cr_2O_3	0.01	<dl	0.10	0.04	0.08	0.04	0.10	0.09	0.05	0.10	<dl
NiO	<dl	<dl	<dl	<dl	<dl	0.08	0.07	<dl	0.03	<dl	0.08
Li_2O*	1.01	0.97	0.94	0.64	0.85	0.99	1.07	0.80	0.95	0.89	0.93
H_2O*	3.64	3.50	3.51	3.64	3.61	3.71	3.80	3.74	3.80	3.70	3.70
Subtotal	101.71	101.25	102.14	99.04	100.03	96.42	97.40	97.77	98.02	98.57	97.94
O=F.Cl	0.29	0.40	0.40	0.20	0.26	0.15	0.10	0.13	0.12	0.18	0.17
Total	101.42	100.85	101.74	98.84	99.77	96.28	97.30	97.64	97.90	98.39	97.78
	Cation proportions are based on 24 oxygens										
Si	5.564	5.565	5.533	5.516	5.561	5.689	5.664	5.560	5.582	5.596	5.637
Al iv	2.436	2.435	2.467	2.484	2.439	2.311	2.336	2.440	2.418	2.404	2.363
Al vi	0.433	0.427	0.380	0.399	0.453	0.497	0.478	0.343	0.393	0.352	0.319
Ti	0.182	0.213	0.139	0.105	0.138	0.273	0.266	0.381	0.312	0.338	0.277
Cr	0.002	<dl	0.012	0.005	0.009	0.005	0.012	0.011	0.006	0.012	<dl
Fe	2.929	2.861	3.037	3.087	2.865	2.119	2.121	2.185	2.081	2.428	2.443
Mn	0.033	0.034	0.020	0.051	0.022	0.023	0.021	0.013	0.021	0.043	0.029
Mg	2.029	2.043	2.128	2.300	2.192	2.439	2.500	2.480	2.611	2.288	2.449
Ni	<dl	<dl	<dl	<dl	<dl	0.010	0.009	<dl	0.004	<dl	0.010
Li*	0.614	0.592	0.571	0.402	0.525	0.615	0.657	0.496	0.582	0.549	0.580
Ca	0.001	0.006	<dl	0.005	0.007	0.003	0.001	0.007	0.003	0.012	0.013
Na	0.011	0.021	0.028	0.014	0.023	0.017	0.014	0.015	0.020	0.010	0.024
K	1.763	1.782	1.736	1.529	1.736	1.869	1.793	1.915	1.924	1.788	1.801
Ba	0.015	0.009	0.015	0.010	0.021	0.011	0.017	0.029	0.003	0.034	0.002
OH*	3.672	3.546	3.541	3.769	3.698	3.831	3.885	3.850	3.864	3.794	3.807
F	0.326	0.453	0.459	0.229	0.302	0.167	0.111	0.150	0.134	0.205	0.191
Cl	0.002	0.001	<dl	0.002	<dl	0.003	0.004	<dl	0.002	0.001	0.001
Sum	20.012	19.989	20.066	19.908	19.992	19.882	19.889	19.875	19.960	19.855	19.947

<dl: below detection limits.

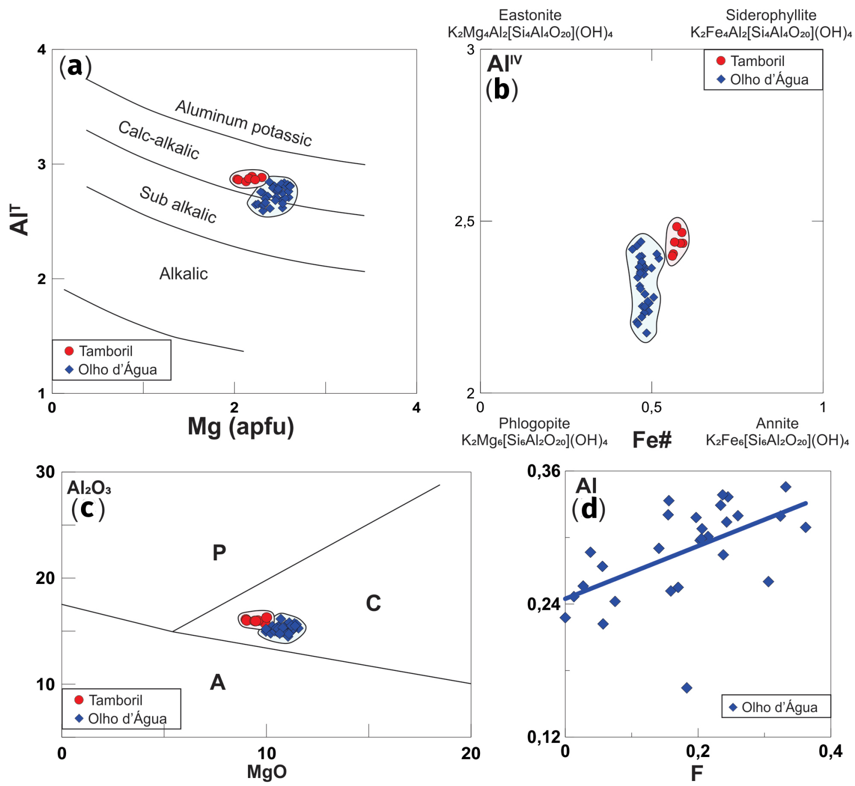

Figure 5. Chemical classification and discrimination diagrams for biotite (a-c): (a) Al^T vs Mg diagram, fields after Nachit et al. (1985); (b) Al^{IV} vs Fe/(Fe+Mg) diagram; (c) Diagram proposed by Abdel-Rahman (1994). Symbols: A = alkalic; C = calc–alkalic; P = peraluminous (Deer et al. 1992); (d) Al vs. F correlation of titanites from the Olho d'Água stock.

in the 500–1000 °C range and the Si contents < 7.8 apfu. Subsequently, Holland & Blundy (1994) proposed a new calibration (HB thermometer) for the edenite-tremolite reaction, which requires silica saturation, and reduced the level of uncertainty from ± 75 °C to ± 35 °C.

Temperature estimates were calculated by both semi-empirical thermometers of Blundy & Holland (1990) and Holland & Blundy (1994) (Table VII), using the compositions where rims of plagioclase and amphibole crystals in contact to each other, i.e. where the two phases are most likely to have been in exchange equilibrium. Estimated temperature using Blundy & Holland (1990) are 675° to 713 °C (average 692 °C, BH) for the Tamboril, and 696° to 744 °C (average 714 °C, BH) for the Olho d'Água pluton (Table VII). Calibration of Holland & Blundy (1994) geothermometer, based on the reaction "edenite + 4 quartz = tremolite + albite" (Fig. 7) requires silica saturation and presence of Ca-amphibole and Na-rich plagioclase, which is the case for both plutons. Estimated temperatures are 587° to 641 °C (average 612 °C, HB) for Tamboril and 637° to 679 °C (average 652 °C, HB) for Olho d'Água. All these calculated temperatures are lower than expected crystallization temperatures of granitic magmas (650° to 700 °C, at 4-10 kbar; Luth et al. 1964) and lower than temperatures calculated by the BH thermometer. Therefore, using both thermometers, temperature results are distinct for both stocks, although with some overlap. The estimated temperatures represent that of the equilibrium crystallization of plagioclase and amphibole, somewhere between liquidus and solidus.

Al–in–hornblende barometry

Anderson & Smith (1995) and Anderson (1996) showed that both temperature and total pressure are sensitive parameters to influence the mineral chemistry of mafic silicates and that all barometers are often affected by variations

Table IV. **Microprobe analyses of epidote from Tamboril (TAM) and Olho d'Água (OA) plutons.**

Sample	BELRS-2A	BELRS-2A	BELRS-10B	BELRS-10B	BELRS-16B	BELRS-16B	BELRS-20B	BELRS-20B	BELRS-31	BELRS-31	BELRS-32
Position	Center	Center	Center	Rim	Center	Rim	Center	Rim	Center	Rim	Center
Pluton	TAM	TAM	TAM	TAM	OA	OA	OA	OA	OA	OA	OA
SiO_2	38.40	39.00	38.38	38.83	37.95	37.93	36.86	36.42	38.17	38.53	36.68
TiO_2	0.11	0.20	0.27	0.15	0.13	0.44	0.01	0.17	0.27	0.82	0.20
Al_2O_3	24.41	26.96	26.65	26.84	25.33	25.81	25.27	24.75	26.42	26.67	23.86
FeO	10.90	7.53	7.91	8.04	9.13	9.07	9.53	10.51	8.32	7.94	10.58
MnO	0.17	0.09	0.13	0.17	0.18	0.19	0.33	0.30	0.15	0.07	0.18
MgO	0.05	<dl	<dl	0.01	<dl	0.03	0.02	0.34	0.02	0.01	0.14
CaO	23.29	23.85	23.47	23.43	23.37	23.13	22.78	22.54	23.26	23.23	22.03
Na_2O	<dl	0.02	<dl	<dl	0.02	0.01	0.04	0.04	0.01	0.02	0.01
K2O	0.02	<dl	0.01	<dl	<dl	<dl	<dl	0.02	0.01	0.01	0.04
BaO	0.10	0.05	0.05	0.02	0.06	0.09	<dl	0.08	0.05	0.05	<dl
F	<dl	<dl	<dl	<dl	<dl	<dl	<dl	<dl	<dl	<dl	<dl
Cl	0.01	0.01	0.01	<dl	<dl	<dl	0.02	<dl	<dl	<dl	<dl
Cr_2O_3	0.09	0.18	0.07	0.11	0.14	0.13	0.16	0.08	0.05	0.15	0.04
NiO	<dl	0.01	0.01	<dl	<dl	0.05	<dl	0.03	<dl	<dl	0.05
V_2O_3	0.06	0.17	0.07	0.11	0.05	0.12	0.04	0.05	0.12	0.16	0.11
Total	97.61	98.07	97.02	97.71	96.35	96.98	95.06	95.31	96.82	97.66	93.93
	Cation proportions are based on 12.5 oxygens										
Si	3.015	3.018	3.005	3.016	3.006	2.984	2.966	2.934	2.997	2.996	2.990
Ti	0.007	0.012	0.016	0.009	0.008	0.026	0.001	0.010	0.016	0.048	0.012
Al	2.259	2.459	2.459	2.456	2.365	2.393	2.396	2.349	2.445	2.443	2.292
Fe^{+3}	0.716	0.487	0.518	0.522	0.605	0.597	0.641	0.708	0.546	0.516	0.721
Mn	0.011	0.006	0.009	0.011	0.012	0.013	0.022	0.021	0.010	0.005	0.013
Mg	0.006	<dl	<dl	0.001	<dl	0.003	0.003	0.040	0.002	0.001	0.017
Ca	1.959	1.978	1.969	1.950	1.984	1.949	1.964	1.946	1.957	1.935	1.924
Na	<dl	0.002	<dl	<dl	0.004	0.001	0.006	0.006	0.001	0.003	0.002
K	0.002	<dl	0.001	<dl	<dl	<dl	<dl	0.002	0.001	0.001	0.004
Ba	0.003	0.002	0.001	0.001	0.002	0.003	<dl	0.002	0.002	0.002	<dl
Cr	0.006	0.011	0.004	0.006	0.009	0.008	0.010	0.005	0.003	0.009	0.003
Ni	<dl	<dl	0.001	<dl	<dl	0.003	<dl	0.002	<dl	<dl	0.004
V	0.004	0.011	0.005	0.007	0.003	0.007	0.002	0.003	0.008	0.010	0.007
Sum	7.987	7.987	7.987	7.979	7.997	7.988	8.012	8.028	7.987	7.969	7.990
Pistacite	24	17	17	18	20	20	21	23	18	17	24

<dl: below detection limits.

Table V. **Microprobe analyses of titanite from the Tamboril (TAM) and Olho d'Água (OA) plutons.**

Sample	**BELRS-21**	**BELRS-14A**	**BELRS-14A**	**BELRS-19A**	**BELRS-19A**	**BELRS-20A**	**BELRS-27**	**BELRS-27**	**BELRS-30**	**BELRS-30**	**BELRS-32**
Position	Rim	Center	Rim	Center	Rim	Center	Center	Rim	Center	Rim	Center
Pluton	TAM	OA	OA	OA	OA	OA	OA	OA	OA	OA	OA
SiO_2	30.54	30.74	31.38	29.58	30.58	32.22	30.10	30.13	29.70	30.24	30.02
TiO_2	36.95	38.52	37.96	41.67	41.20	37.54	42.00	40.93	41.85	42.02	41.20
Al_2O_3	2.19	1.89	2.21	1.49	1.61	1.67	2.26	2.09	1.62	1.52	1.46
FeO	0.67	0.52	0.54	0.52	0.60	0.54	0.58	0.89	0.49	0.58	0.54
MnO	0.03	0.09	0.11	0.09	0.09	0.09	0.11	0.01	<dl	0.10	0.10
MgO	0.01	<dl	0.01	<dl	<dl	<dl	0.03	0.27	<dl	0.03	0.01
CaO	27.08	27.84	28.02	26.54	27.36	27.20	27.03	27.16	27.09	27.80	27.02
Na_2O	0.08	0.02	0.01	0.02	0.01	0.02	0.02	0.05	0.02	0.01	<dl
K_2O	<dl	<dl	0.01	<dl	0.01	<dl	<dl	0.10	<dl	0.01	0.01
BaO	0.13	0.15	0.19	<dl	0.35	<dl	0.02	0.12	<dl	0.10	0.01
F	0.34	0.14	0.25	<dl	0.08	0.17	0.24	0.24	0.01	0.18	0.06
Cl	0.01	<dl	<dl	<dl	<dl	0.01	0.01	<dl	0.01	<dl	<dl
Cr_2O_3	0.04	0.07	0.14	0.01	<dl	0.06	0.07	0.08	<dl	<dl	0.04
NiO	0.03	0.03	0.09	<dl	<dl	<dl	<dl	0.04	<dl	0.02	<dl
V_2O_3	0.30	0.36	0.26	0.22	0.25	0.30	0.31	0.44	0.37	0.34	0.31
Total	98.24	100.32	101.09	100.14	102.09	99.75	102.68	102.45	101.15	102.87	100.76
	Cation proportions are based on 20 oxygens										
Si	4.053	3.999	4.049	3.848	3.912	4.184	3.823	3.848	3.829	1.914	3.885
Ti	3.689	3.770	3.684	4.079	3.965	3.668	4.013	3.932	4.059	2.030	4.011
Al	0.342	0.290	0.337	0.228	0.242	0.255	0.338	0.314	0.247	0.164	0.222
Fe^{+2}	0.075	0.056	0.059	0.057	0.064	0.059	0.062	0.095	0.053	0.053	0.058
Mn	0.003	0.010	0.012	0.010	0.010	0.010	0.012	0.001	<dl	<dl	0.011
Mg	0.002	<dl	0.003	<dl	<dl	<dl	0.006	0.051	<dl	<dl	0.002
Ca	3.850	3.880	3.873	3.700	3.751	3.786	3.678	3.717	3.742	3.742	3.747
Na	0.021	0.006	0.003	0.006	0.003	0.006	0.005	0.013	0.004	0.008	0.001
K	<dl	<dl	0.001	<dl	0.001	<dl	<dl	0.017	<dl	<dl	0.002
Ba	0.007	0.008	0.010	<dl	0.018	<dl	0.001	0.006	<dl	<dl	0.001
Cr	0.004	0.007	0.014	0.001	<dl	0.006	0.007	0.008	<dl	<dl	0.004
Ni	0.003	0.003	0.009	<dl	<dl	<dl	<dl	0.004	<dl	<dl	<dl
V	0.031	0.038	0.027	0.023	0.025	0.031	0.032	0.045	0.038	0.025	0.032
Sum	12.080	12.066	12.080	11.950	11.991	12.005	11.978	12.050	11.972	7.937	11.976

<dl: below detection limits.

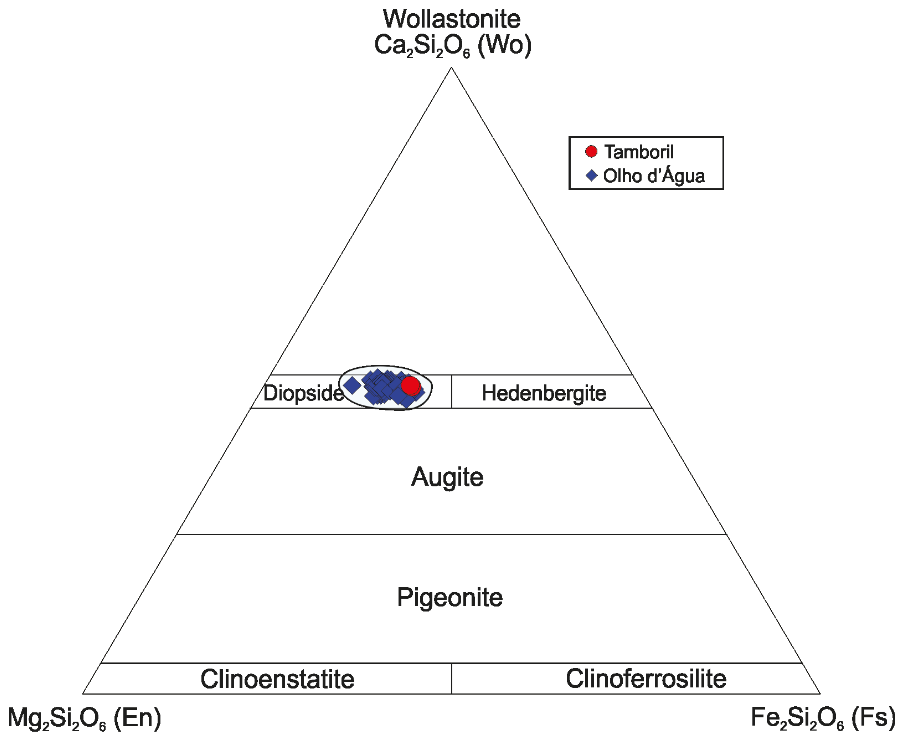

Figure 6. Compositional variation diagram as a function of the molecular components Wo, En and Fs of pyroxenes from the Tamboril and Olho D´Água plutons (Morimoto 1988).

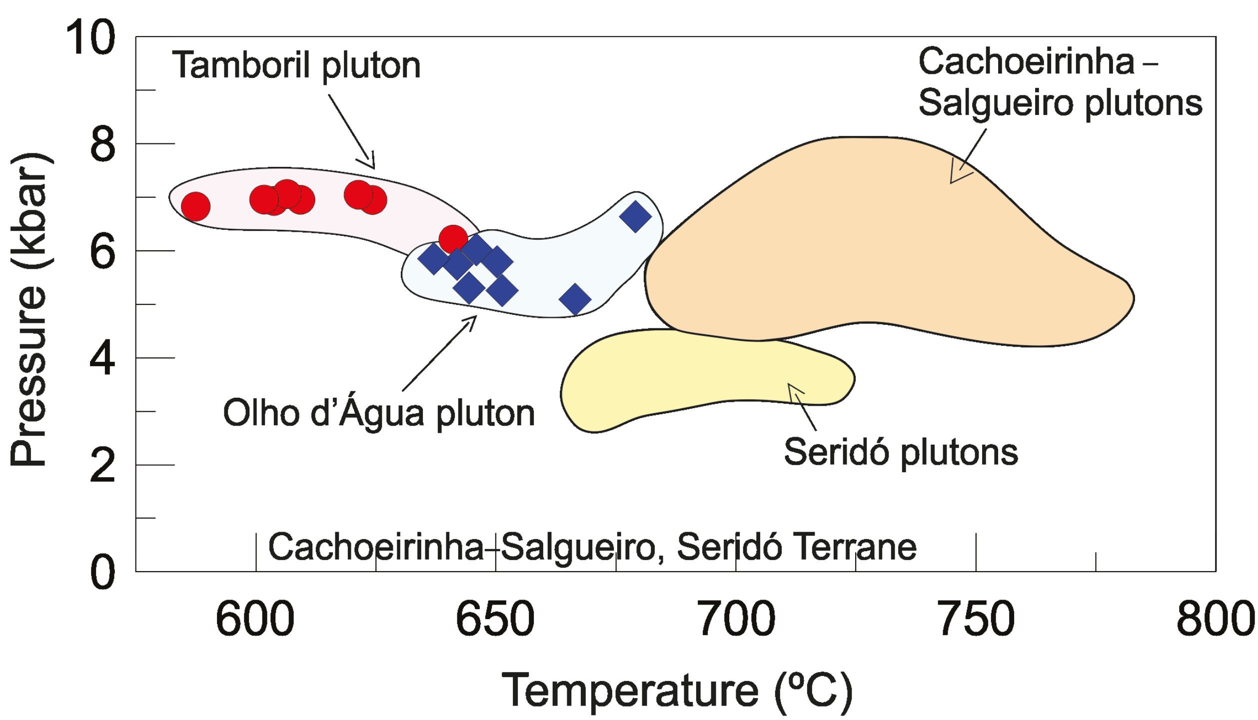

Figure 7. Thermobarometry of Tamboril and Olho d'Água plutons. The regions with orange and yellow colors are the data obtained in plutons analyzed by Sial et al. (1999) in the Cachoeirinha–Salgueiro and Seridó terranes. See text for details.

in intensive parameters such as oxygen fugacity. They have shown that at low oxygen fugacity the barometer fails to record high pressure (as known from independent evidence) for plutons with iron–rich hornblende coexisting with the full barometric assemblage (quartz, iron–magnesium silicates, euhedral titanite and magnetite). Therefore, the barometer is recommended for hornblende Fe/(Fe+Mg) ratio with values between 0.40 and 0.65.

The Anderson & Smith (1995) barometer was applied in this study. This Al-in-hornblende barometer is dependent on temperature, which in this study was that calculated using the thermometer proposed by Holland & Blundy (1994) as discussed above. These results are shown in Table VII and in Figure 7. The pressure ranges obtained are distinct for the two stocks. In the Tamboril pluton, the pressure values are between 6.2 and 7.0 kbar (average 6.9 kbar), while in the Olho d'Água pluton pressure values are between 5.1 and 6.6 kbar (average 5.7 kbar).

For comparison, the Mutch et al. (2016) barometer, which is based only on the total Al, was also calculated (Table VII). These authors caution that their barometer is valid in the range of T = 725 ± 75°C, which are temperatures substantially higher than our calculated temperatures (except for Olho D´Água stock). Values of pressure calculated by the Mutch et al. (2016) barometer are between 4.9 and 5.2 kbar (Tamboril pluton) and and between 3.8 and 5.3 kbar (Olho d'Água pluton).

So, serious discrepancies pertain to pressures calculated by the two barometers based upon the same data. Temperatures determined by the hornblende-plagioclase pair seem to have been affected by solidus re-equilibration, especially in the Tamboril pluton, where they are lower than the temperature range required for use of Mutch's barometer. Therefore, one assumes here that only pressures estimated for the Olho d'Água pluton should be considered for further discussion.

Near-liquidus temperature estimates using Zr saturation thermometry

If a granitic melt is saturated with Zr, the whole-rock abundance of Zr is related to the temperature of zircon crystallization (Watson 1987). Watson & Harrison (1983) demonstrated that zircon saturation thermometry provides a simple and consistent means of estimating magma temperatures, and showed experimentally that the solubility of zircon is correlated with magmatic SiO_2 contents. Zircon must be the first mineral to crystallize, and solely of magmatic origin (not inherited and not a cumulate phase). According to this methodology, a minimum liquidus temperature can be calculated by the equation of Watson & Harrison (1983) as rearranged by Miller et al. (2003) using the Zr of the total rock (ppm):

$$T_{Zr} = \frac{12900}{2.95 + 0.85M + \ln\left(496000/Zr_{melt}\right)}.$$

Results for the Tamboril stock range from 807 to 829 °C, and for the Olho d'Água stock between 788 and 819 °C (Table VIII). Fig. 8 summarizes T-P relationships; it displays an estimated near-liquidus temperature for mEp-bearing plutons in the region, and an H_2O-saturated solidus in relation to calculated intensive data for the Tamboril and Olho d'Água plutons.

These calculated near liquidus temperature are similar to the range of those estimated using the method of apatite saturation of Green & Watson (1982), between 800°C and 900°C as illustrated in the Fig. 3a, as well as using the relationship TiO_2 and silica contents (Green & Pearson 1986) that indicates T< 900°C (Fig. 3b).

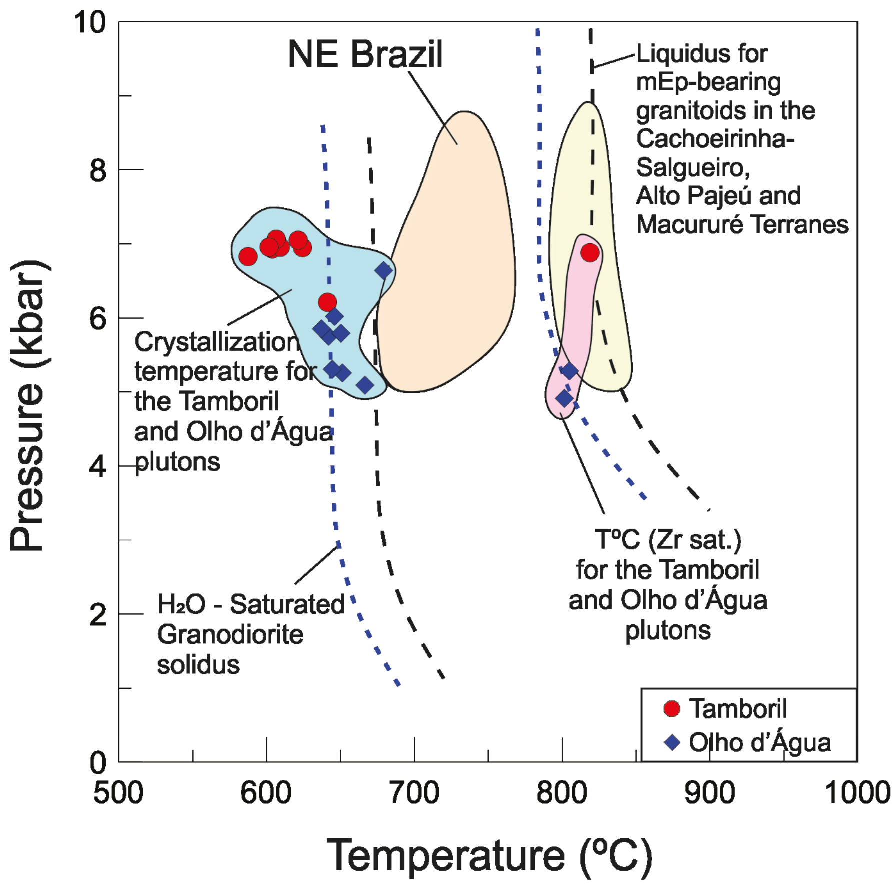

Figure 8. P–T diagram for granitoids with magmatic epidote of the Cachoeirinha–Salgueiro Terrane. Curve of the liquidus obtained with the zircon saturation equation and curve for the solidus (magmatic curve for H_2O saturated granitoids). The regions with light orange and light yellow are P-T of plutons studied by Sial et al. (1999), the light blue region temperature and pressure of crystallization of the Tamboril and Olho d'Água plutons, and the region in pink are near- liquidus temperature and pressure of these plutons.

DISCUSSION

Source rock

Silica contents of the studied rocks range from ~63.7 to 67.9 wt% in the Tamboril pluton and from ~62.1 to 65.1 wt% in the Olho d'Água pluton (Siqueira et al. 2018). Samples from the two plutons form almost continuous, although distint groups, in silica vs. oxide diagrams, as illustrated for the correlation between silica and P_2O_5 and TiO_2 (Figs 3a, 3b).

Granitic/granodioritic magmas are usually considered to have formed from evolution of basaltic magmas or by crustal anatexis (e.g. Jagoutz 2010, Brown 1994, 2013, and references therein). Neverthless, experiments show that granitic/granodioritic magmas can be produced from dehydration of amphibolites (e.g. Beard & Lofgren 1991, Rushmer 1991, Rapp & Watson 1995, Douce 1999) or from basaltic compositions (e.g. Beard & Lofgren 1991, Sisson et al. 2005). Several lines of evidence suggest that the studied rocks derived from magmas formed from melting of mafic rocks. For instance, major element compositions of the studied plutons are similar to those of experimentally-obtained melts from amphibolites studied by Douce (1999) (Fig. 3c). Besides, the widespread presence of amphibole-rich mafic clots, as well as diorite enclaves in the studied plutons are suggestive of a source derivation. One of the type of amphibole-rich clots presents an external layer of biotite + amphibole surrounding actinolite with magnesio-hornblende margins (Fig. 2d). Usually this type of ARC show angular shape (Fig. 2c) suggesting that they were captured as solid by the tonalite magma. The mafic enclaves are commonly found in the rocks of both plutons.

Table VI. **Microprobe analyses of clinopyroxene from Tamboril (TAM) and Olho d'Água (OA) plutons.**

Sample	BELRS-2A	BELRS-2A	BELRS-13A	BELRS-13A	BELRS-16A	BELRS-16A	BELRS-19A	BELRS-19A	BELRS-19D	BELRS-19D	BELRS-25	BELRS-25	BELRS-32	BELRS-32
Position	Center	Rim	Center	Rim	Center	Rim	Center	Rim	Center	Rim	Center	Rim	Center	Rim
Pluton	TAM	TAM	OA	OA	OA	OA	OA	OA	OA	OA	OA	OA	OA	OA
SiO_2	52.80	53.09	51.47	51.93	53.66	53.14	52.48	52.09	55.72	55.52	52.74	52.20	52.86	52.95
TiO_2	0.26	0.25	0.44	<dl	<dl	0.03	0.19	<dl	0.02	0.08	0.08	0.05	0.16	<dl
Al_2O_3	0.79	0.79	1.35	0.46	0.71	0.57	0.81	0.92	0.67	0.72	1.18	0.59	0.67	0.94
Cr_2O_3	<dl	<dl	0.05	<dl	0.11	0.08	0.07	0.13	0.12	0.01	<dl	<dl	0.12	0.02
FeO	12.01	11.79	12.88	12.35	10.41	9.97	9.71	9.93	9.38	9.74	11.55	11.27	12.36	11.82
MnO	0.38	0.36	0.44	0.43	0.34	0.43	0.32	0.41	0.42	0.50	0.30	0.50	0.55	0.39
MgO	10.32	10.36	10.29	10.68	12.53	12.55	11.72	11.56	11.45	11.25	10.36	10.58	11.10	11.47
CaO	22.77	22.90	22.38	23.41	23.22	22.94	22.80	22.27	23.02	23.08	23.10	22.96	22.20	22.70
Na_2O	0.26	0.43	0.40	0.38	0.30	0.27	0.35	0.38	0.44	0.48	0.44	0.39	0.29	0.38
K_2O	0.02	<dl	<dl	<dl	<dl	0.01	0.01	<dl	0.03	<dl	<dl	<dl	0.01	<dl
Total	99.61	99.96	99.71	99.65	101.27	99.99	98.46	97.68	101.28	101.36	99.75	98.53	100.31	100.67
	Cation proportions are based on 6 oxygens													
Si	2.019	2.019	1.967	1.980	1.993	1.997	2.007	2.008	2.074	2.067	2.006	2.009	2.003	1.990
Ti	0.007	0.007	0.013	<dl	<dl	0.001	0.005	<dl	0.001	0.002	0.002	0.001	0.005	<dl
Al	0.036	0.035	0.061	0.020	0.031	0.025	0.037	0.042	0.029	0.031	0.053	0.027	0.030	0.041
Fe^{+3}	<dl	<dl	0.009	0.047	0.002	<dl	<dl	<dl	<dl	<dl	<dl	<dl	<dl	0.006
Cr^{+3}	<dl	<dl	0.001	<dl	0.003	0.002	0.002	0.004	0.004	<dl	<dl	<dl	0.003	0.001
Fe^{+2}	0.384	0.375	0.403	0.347	0.322	0.313	0.310	0.320	0.292	0.303	0.368	0.363	0.392	0.365
Mn	0.012	0.011	0.014	0.014	0.011	0.014	0.010	0.014	0.013	0.016	0.010	0.016	0.018	0.013
Mg	0.588	0.587	0.586	0.607	0.693	0.703	0.668	0.664	0.636	0.624	0.587	0.607	0.627	0.643
Ca	0.933	0.933	0.916	0.957	0.924	0.924	0.934	0.920	0.918	0.921	0.942	0.947	0.901	0.914
Na	0.019	0.032	0.030	0.028	0.022	0.020	0.026	0.028	0.032	0.035	0.032	0.029	0.021	0.028
K	0.001	<dl	<dl	<dl	<dl	0.001	0.001	<dl	0.002	<dl	<dl	<dl	<dl	<dl
Sum	4.000	4.000	4.000	4.000	4.000	4.000	4.000	4.000	4.000	4.000	4.000	4.000	4.000	4.000
Wo	48.97	49.22	48.09	50.06	47.65	47.60	48.84	48.30	49.75	49.82	49.65	49.40	46.94	47.56
En	30.87	30.99	30.77	31.78	35.77	36.25	34.94	34.89	34.43	33.78	30.97	31.67	32.66	33.44
Fs	20.16	19.79	21.14	18.16	16.58	16.15	16.23	16.81	15.82	16.40	19.38	18.93	20.40	19.00

<dl: below detection limits.

Usually thet have sharp contacts with the host rocks, although they tend to have elliptical to rounded shapes. They are mainly fine-grained dioritic rocks, including diorite and pyroxene diorite with igneous textures, and having condensing edges with rich fine dark minerals.

Similar features are observed in many other plutons of this type in the Cachoeirinha-Salgueiro Terrane (e.g. Sial & Ferreira 2015) in the mafic clots (chiefly calcic amphibole, plus clinopyroxene, biotite, euhedral titanite) are interpreted to be fragments, possibly restites, from partial fusion of amphibolitic source (Sial & Ferreira 2015). The mafic fragments could have been transported upward by granodiorite/tonalite magmas from a metabasaltic source to crystallize at shallower depth (Sial 1993, Sial et al. 1998, 2008, Ferreira et al. 2003, 2011). This way,

Table VII. Summary of the estimation of crystallization conditions from Tamboril and Olho d'Água Plutons.

Sample	Belrs-2A	Belrs-2A	Belrs-2A	Belrs-2A	Belrs-2A	Belrs-2A	Belrs-2A	Belrs-2A	Belrs-13A	Belrs-13A	Belrs-31	Belrs-31	Belrs-31	Belrs-31	Belrs-31	Belrs-31
Pluton	TAM	TAM	TAM	TAM	TAM	TAM	TAM	TAM	OA	OA	OA	OA	OA	OA	OA	OA
T1 (H&B. 1994)	587.4	603.7	609.3	606.5	624.3	641.1	601.7	621.4	666.5	679.1	641.9	645.9	651.3	637.0	644.4	650.2
P(T1) (A&S. 1995)	6.83	6.93	6.95	7.06	6.95	6.21	6.95	7.05	5.09	6.64	5.75	6.02	5.26	5.85	5.31	5.79
P (Mutch. 2016)	4.90	5.02	5.05	5.13	5.11	4.59	5.03	5.18	3.88	5.31	4.23	4.47	3.91	4.29	3.91	4.32
T2 (H&B. 1994)	597.0	616.2	618.1	604.7	634.8	652.9	617.5	621.8	683.5	682.6	655.7	665.9	647.7	638.2	671.1	662.3
P(T2) (A&S. 1995)	6.81	6.88	6.91	7.07	6.88	6.11	6.89	7.05	4.91	6.59	5.64	5.84	5.28	5.84	5.08	5.68
T3 (B&H. 1990)	675.0	687.0	687.8	686.3	704.4	713.0	688.7	697.1	719.2	744.7	711.1	717.4	694.5	696.8	716.3	712.8
P(T3) (A&S. 1995)	6.24	6.22	6.24	6.35	6.06	5.35	6.21	6.25	4.42	5.50	4.97	5.14	4.81	5.24	4.50	5.04

Temperature in °C calculated: T1 (Holland & Blundy 1994) refers to Holland & Blundy (1994) reaction A, T2 (Holland & Blundy 1994) refers to Holland & Blundy (1994) reaction B, T3 (Blundy & Holland 1990) refers to Blundy & Holland (1990) thermometry. P(T1)-P(T2)-P(T3) (Anderson & Smith 1995) refers to Anderson & Smith (1995) Al-in-hornblende barometry for each temperature calculated. P (Mutch 2016) refers to Mutch et al. (2016) barometry. Belrs-2A – Tamboril Pluton. Belrs-13A and Belrs-31 – Olho d'Água Pluton.

we infer a similar source for the magmas that originated the studied plutons, and a similar mechanism of fragment transportation.

Low whole-rock magnetic susceptibility (≈ 0.3×10^{-3} SI) reported by Siqueira et al. (2018) for the studied stocks is compatible with an S–type origin for the magmas (Chappell & White 1974), but within the range for ilmenite-series of granitoids (Ishihara 1977, 1998, Takahashi et al. 1980). Nevertheless, Sial et al. (1999) identified magmatic epidote-bearing granites in the Cachoeirinha–Salgueiro Terrane that have low magnetic susceptibility (<0.5 × 10^{-3} SI) , and interpreted them to be I-type rocks. They attributed this low magnetic susceptibility for I-type granite as due to incorporation of Fe^{+3} into epidote rather than into iron oxide minerals. In fact, Schmidt & Thompson (1996) noted that magnetite is more abundant in epidote-free granites than in epidote-bearing granites (2.1–18 kbar and 550–850 °C).

Magmatic crystallization

Inclusion-free euhedral clinopyroxene grains are interpreted here as crystallized from the host tonalite magma, whereas inclusion-rich subhedral grains in diorite enclaves are interpreted as residues from the magma source. Thompson & Ellis (1994) proposed that during melting, epidote + amphibole + quartz can produce liquid + clinopyroxene at T >800 °C and P between 10 and 25 kbar. Long et al. (2005) proposed that during dehydration-melting of an amphibolitic source rock, amphibole-rich clots + clinopyroxene could produce melt + residual clinopyroxene. Dehydration melting reactions can produce clinopyroxene at the expense of biotite and amphibole (e.g., Chappell et al. 2012).

Titanite in the Olho d'Água pluton tends to be enriched in Al and F, which suggests crystallization at moderate to high pressure (Erdmann et al. 2019; Evans & Patrick 1987, Franz & Spear 1985, Tropper et al. 2002). The Mg/(Mg+Fe) ratios (0.45–0.70) in amphibole are consistent with the range proposed by Mason (1985) for calc–alkalic granitoids, while Fe/(Fe+Mg) ratios indicate moderately high oxygen fugacity at crystallization of this phase.

Textural criteria to recognized primary epidote includes euhedral to subhedral grains with allanite core and oscillatory zoning (e.g. Sial 1990) similar to the ones shown in the studied plutons (Fig. 2g, 2h). Chemical criteria to distinguish magmatic epidote on the other hand

Table VIII. Estimated near-liquidus temperature using Zr-saturation equation of Watson & Harrison (1983) rearranged by Miller et al. (2003). Zr concentration in ppm.

Sample	Zr	T (°C)
(A) Tamboril Pluton		
BELRS-02	227	819
BELRS-06	233	829
BELRS-06A	211	822
BELRS-07	194	807
BELRS-08	226	824
BELRS-09	233	818
BELRS-10B	215	827
BELRS-21	200	826
BELRS-21M	214	814
(B) Olho d'Água Pluton		
BELRS-04A	200	801
BELRS-04B	206	805
BELRS-05	211	800
BELRS-13	208	802
BELRS-14	207	808
BELRS-16	193	790
BELRS-17	201	788
BELRS-18	224	804
BELRS-19A	205	806
BELRS-19B	202	797
BELRS-20	192	790
BELRS-25	204	804
BELRS-26	197	808
BELRS-27	214	802
BELRS-28	212	804
BELRS-29	248	818
BELRS-30	213	804
BELRS-31	215	805
BELRS-32	242	819

is based on either pistacite content of epidote (Ps = molar $[Fe^{3+}/(Fe^{3+}+Al)]100$)>25%, (Tulloch 1979), or on TiO_2 contents, as suggested by Evans and Vance (1987), for whom magmatic epidote typically has < 0.2 wt% TiO_2, whereas secondary epidote that is a replacement of biotite has > 0.6

wt% TiO_2. Epidote compositional variation from the Tamboril (Ps_{17-20}) and Olho d'Água (Ps_{18-26}) plutons are slightly below the values proposed by Tulloch (1979) for typically magmatic epidote (Ps_{25} to Ps_{29}), and would suggest that these epidote formed from alteration of plagioclase. However, these pistacite contents are close to the range of pistacite reported as typical for mEp (Ps_{20-25}) by Sial (1990), Sial et al. (1998), Brasilino et al. (2011) and Sial & Ferreira (2015), for Ediacaran granitoids in the Cachoeirinha–Salgueiro Terrane. Despite the slightly lower pistacite contents, Sial et al. (2008) interpreted euhedral to subhedral epidote crystals rimmed by biotite, with zoned allanite core as typical of magmatic epidote in the Cachoeirinha–Salgueiro Terrane (Sial et al. 2008, Ferreira et al. 2011, Sial & Ferreira 2015).

In samples from the two studied plutons in which clinopyroxene occur together with epidote, pyroxene is less abundant than epidote, as also observed in the Pedra Branca pluton, a similar calc-alkalic mEp granite (Sial & Ferreira 2015). These authors interpret the relation between clinopyroxene and epidote as consistent with Schmidt & Thompson (1996) experiments on water–saturated tonalitic magmas, which shows that the appearance of clinopyroxene occurs at the expense of epidote according to the reaction clinopyroxene + liquid = epidote + hornblende + H_2O, and so epidote increases at the expense of clinopyroxene.

Granitoid magmas have been classified into magnetite series (high fO_2) and ilmenite series (low fO_2) (Ishihara 1977). The boundary separating these series is between the HM and FMQ buffers (Wones 1989). Oxygen fugacity relates to magma source, a critical controlling parameter of magmatic processes. Although it is difficult, on the basis of an evolved final product (granite) to infer the oxygen fugacity of primary magma, some T and P conclusions may be used for mineral chemistry and mineral rock assemblage (Enami et al. 1993). Several line of evidence indicate that the Tamboril and Olho D´Água magma was oxidized. Among them are the presence of quartz, amphibole-rich clots, primary biotite, primary epidote (that carries Fe^{3+}) and euhedral titanite, that together imply a relatively oxidized, silica-saturated host magma. Besides the pistacite contents in the epidote of the two plutons in this study and Fe# contents of biotite are consistent with crystallization between FMQ and HM buffers (Sial & Ferreira 2015). On the other hand, biotite from the Tamboril stock exhibits slightly higher Fe#, corresponding to biotite crystallization under slightly lower oxygen fugacity, than biotite from the Olho D´Água stock. The difference in the fO_2 conditions between Tamboril and Olho d'Água magmas may be associated with different magmatic pulses extracted from the same source or with the evolution of two distinct magmas...

Estimated temperature for the Tamboril (587-641°C) and Olho d'Água (637-679°C) stocks, both using Holland & Blundy (1994) are lower than those expected for crystallization temperature of granitic magmas (650° to 700 °C, at 4-10 kbar; Luth et al. 1964). These rather low temperature could be explained by aluminum reequilibration between coexisting amphibole and plagioclase during sub-solidus cooling (e.g. Ferreira et al. 2011). Another possibility is that mineral chemistry in both stocks have changed during magma intrusion into the phyllites of Cachoeirinha-Salgueiro Terrane. Many plagioclase grains in both stocks show alteration suggesting interaction with fluids.

Estimated pressure of crystallization using the Al^t-in-hornlende geobarometer of Anderson & Smith (1995) for the Tamboril stock ranges from 6.2 to 7 kbar while that from the Olho d'Água stock varies from 5.1 to 6.6 kbar. These values are higher than those calculated using

Mutch et al. (2016) barometer (4.9 to 5.2 kbar for the Tamboril pluton, and from 3.8 to 5.3 kbar for the Olho d'Água pluton). The higher pressure estimated using Anderson & Smith (1995) barometer is compatible with the presence of magmatic epidote in the studied rocks, which is indicative of high pressure of crystallization, as suggested by Schmidt & Thompson (1996) who demonstrated experimentally that epidote and plagioclase can coexist around 10 kbar in tonalitic magmas.

Oscillatory textural and compositional zoning are observed in plagioclase grains of the studied plutons (Fig. 2a, 2b). Oscillations in chemical composition are apparently incompatible with slow, near-equilibrium growth (e.g. Shore & Fowler 1995). Many authors interpret this type of zoning as representing changes in temperature during feldspar growth possibily due to magma convection or to eventual reheating of the chamber by replenishment by more mafic magma (e.g. Mariano & Sial 1988, Shcherbakov et al. 2011). This evidence together with presence of biotite rows in plagioclase megacrysts (Fig. 2a) suggest that plagioclase crystallization occurred in a convective magma chamber probably due injection of mafic magma pulses.

Altogether, our data suggest that the studied plutons resulted from crystallization from different magmatic pulses, formed from fractional melting of a single source. These two magma pulses underwent subsequent crystallization, in a convective magmatic chamber, at rather high pressure.

CONCLUSIONS

Our data indicate that the rocks that compose the Tamboril and Olho D´Água stocks are calc-alkalic, metaluminous tonalite to granodiorite, that carry magmatic epidote and diopside, probably formed from crystallization of a magma derived from partial melting of amphibolitic source. The two plutons represent crystallization of two different magma pulses, in a convective magma chamber at intermediate to high oxygen fugacity conditions. Crystallization occurred under rather high pressure, as suggested by presence of magmatic epidote and Al-in-hornblende geobarometer. These two plutons are similar to many other magmatic epidote-bearing granitoids intrusive in the low-grade metapelites, and formed in magmatic-arc setting.

Acknowledgments

We thank Prof. Nilson Botelho (University of Brasilia) for permitting us to use the electron microprobe laboratory of that University. ANS acknowledges grants from FACEPE (APQ 1073-1.07/15) and Conselho Nacional de Desenvolvimento Científico e Tecnológico (CNPq, 407171/2018-5) and VPF, a grant from CNPq (471034/2012-6) which helped defraying costs of this study. We are grateful to two anonymous reviewers whose comments and suggestions greatly contributed to improve our original text. This is the NEG-LABISE contribution n. 292.

REFERENCES

ABDEL RAHMAN AM. 1994. Nature of biotites from alkalic, calc–alkalic, and Peraluminous magmas. J Petrol 35: 525-541.

ANDERSON JL. 1996. Status of thermobarometry in granitic batholiths. Transactions of the Royal Society of Edinburg. Earth Sci 87: 125-138.

ANDERSON JL & SMITH DR. 1995. The effects of temperature and fO_2 on the Al-in-hornblende barometer. Am Mineral 80: 549-559.

BEARD JS & LOFGREN GE. 1991. Dehydration melting and water-saturated melting of basaltic and andesitic greenstones and amphibolites at 1, 3, and 6-9 kb. J Petrol 32: 365-401.

BRASILINO RG, SIAL AN, FERREIRA VP & PIMENTEL MM. 2011. Bulk rock and mineral chemistries and ascent rates of high-K calc-alkalic epidote-bearing magmas, Northeastern Brazil. Lithos 27: 441-454.

BLUNDY J & HOLLAND T. 1990. Calcic amphibole equilibria and a new amphibole-plagioclase geothermometer. Contrib Mineral Petr 104: 208-224.

BROWN M. 1994. The generation, segregation, ascent and emplacement of granite magma: the migmatite-to crustally-derived granite connection in thickened orogens. Earth Sci Rev 36: 83-130.

BROWN M. 2013. Granite: From genesis to emplacement. Geol Soc Am Bull 125: 1079-1113.

CHAPPELL BW & WHITE AJR. 1974. Two contrasting granite types. Pacif Geol 8: 173-174.

CHAPPELL BW, BRYANT CJ & WYBORN D. 2012. Peraluminous I-type granites. Lithos 153: 142-153.

DEER WA, HOWIE RA & ZUSSMAN J. 1992. An introduction to the rock-forming minerals. 2nd ed., Harlow, Longman, 696 p.

DOUCE AEP. 1999. What do experiments tell us about the relative contributions of crust and mantle to the origin of granitic magmas? Geol Soc, London, Special Publications 168(1): 55-75.

ERDMANN S, WANG R, HUANG F, SCAILLET B, ZHAO K, LIU H, CHEN Y & FAURE M. 2019. Titanite: A potential solidus barometer for granitic magma systems. C R Geosci 351(8): 551-561.

ENAMI M, SUZUKI K, LIOU JG & BIRD DK. 1993. Al-Fe^{3+} and F-OH substitutions in titanite and constraints on their P-T dependence. Eur J Mineral 5: 219-231.

EVANS BW & VANCE JA. 1987. Epidote phenocrysts in dacitic dikes, Boulder County, Colorado. Contrib Mineral Petr 96(2): 178-185.

EVANS BW & PATRICK BE. 1987. Phengite-3T in high-pressure metamorphosed granitic orthogneisses, Seward Peninsula, Alaska. Can Mineral 25: 141-158.

FERREIRA VP, SIAL AN & WHITNEY JA. 1994. Large-scale silicate liquid immiscibility: a possible example from northeastern Brazil. Lithos 33(4): 285-302.

FERREIRA VP, SIAL AN, LONG L & PIN C. 1997. Isotopic signatures of Neoproterozoic to Cambrian ultrapotassic syenitic magmas, Northeastern Brazil: implications for enriched mantle source. Int Geol Rev 39: 660-669.

FERREIRA VP, SIAL AN & JARDIM DE SÁ EF. 1998. Geochemical and isotopic signatures of Proterozoic granitoids in terranes of Borborema structural province, northeast Brazil. J S Am Earth Sci 11: 439-455.

FERREIRA VP, VALLEY JW, SIAL AN & SPICUZZA M. 2003. Oxygen isotope compositions and magmatic epidote from two contrasting metaluminous granitoids, NE Brazil. Contrib Mineral Petr 145: 205-216.

FERREIRA VP, SIAL AN, PIMENTEL MM & MOURA CAV. 2004. Intermediate to acidic magmatism and crustal evolution in the Transversal Zone, Northeastern Brazil. Geologia do Continente Sul-Americano: a evolução da obra de Fernando Flávio Marques de Almeida. University of São Paulo, capítulo XII, 189-201.

FERREIRA VP. 2010. Plutonismo saturado a supersaturado na Zona Transversal, porção leste da Província Borborema: revisão petrológica, geoquímica e istópica. Federal University of Pernambuco, Full Professor thesis, 163 p. (Unpublished).

FERREIRA VP, SIAL AN, PIMENTEL MM, ARMSTRONG R, SPICUZZA M, GUIMARÃES I & SILVA FILHO AF. 2011. Contrasting sources and P-T crystallization conditions of epidote-bearing granitic rocks, Northeastern Brazil: O, Sr and Nd isotopes. Lithos 121: 189-201.

FRANZ G & SPEAR ES. 1985. Aluminous titanite (sphene) from the eclogite-zone, south central Tauern Window, Austria. Chem Geol 50: 33-46.

GREEN TH & WATSON EB. 1982. Crystallization of apatite in natural magmas under high pressure, hydrous conditions, with particular reference to ‘orogenic’ rock series. Contrib Mineral Petr 79(1): 96-105.

GREEN TH & PEARSON NJ. 1986. Ti-rich accessory phase saturation in hydrous mafic-felsic compositions at high P, T. Chem Geol 54(3-4): 185-201.

HAMMARSTROM JM & ZEN EA. 1986. Aluminum in hornblende: an empirical igneous geobarometer. Am Mineral 71: 1297-1313.

HOLLAND T & BLUNDY J. 1994. Non-ideal interactions in calcic amphiboles and their bearing on amphibole-plagioclase thermometry. Contrib Mineral Petr 116(4): 433-447.

ISHIHARA S. 1977. The magnetite-series and ilmenite-series granitic rocks. Min Geol 27: 293-305.

JAGOUTZ OE. 2010. Construction of the granitoid crust of an island arc. Part II: a quantitative petrogenetic model. Contrib Mineral Petr 160: 359-381.

ISHIHARA S. 1998. Granitoid Series and Mineralization in the Circum-Pacific Phanerozoic Granitic Belts. Resour Geol 48(4): 219-224.

LEAKE BE ET AL. 1997. Nomenclature of amphiboles; report of the Subcommittee on Amphiboles of the International Mineralogical Association Commission on new minerals and mineral names. Mineral Mag 61(405): 295-310.

LONG LE, CASTELLANA CH & SIAL AN. 2005. Age, Origin and Cooling History of the Coronel João Sá Pluton, Bahia, Brazil. J Petrol 46(2): 255-273.

LUTH WC, JAHNS RH & TUTTLE OF. 1964. The granite system at pressures of 4 to 10 kilobars. J Geophys Res 69(4): 759-773.

MARIANO G & SIAL AN. 1988. Evidence of magma mixing in the Itaporanga batholith Northeastern Brazil. Rendic. Soc Ital Mineral Petrol 43: 555-567.

MASON GH. 1985. The mineralogy and textures of the Coastal Batholith, Peru. In: Pitcher WS, Atherton MP, Cobbing EJ & Beckinsale RD (Eds), Magmatism at a Plate Edge: The Peruvian Andes. Blackie Halstead Press, Glasgow: 156-166.

MILLER CF, MCDOWELL SM & MAPES RW. 2003. Hot and cold granites? Implications of zircon saturation temperatures and preservation of inheritance. Geology 31(6): 529-532.

MORIMOTO N. 1988. Nomenclature of pyroxenes. Miner Petrol 39(1): 55-76.

MUTCH EJF, BLUNDY JD, TATTITCH BC, COOPER FJ, & BROOKER RA. 2016. An experimental study of amphibole stability in low-pressure granitic magmas and a revised Al-in-hornblende geobarometer. Contrib Mineral Petr 171(10): 1-27.

NACHIT H, RAZAFIMAHEFA N, STUSSI JM & CARRON JP. 1985. Composition chimique des biotites et typologie magmatique des granitos. CR Acad Sci Paris 301: 810-818.

RAPP RP & WATSON EB. 1995. Dehydration melting of metabasalt at 8-32 kbar: implications for continental growth and crust-mantle recycling. J Petrol 36(4): 891-931.

RUSHMER T. 1991. Partial melting of two amphibolites: contrasting experimental results under fluid-absent conditions. Contrib Mineral Petr 107: 41-59.

SCHMIDT MW & THOMPSON AB. 1996. Epidote in calc-alkalic magmas: an experimental study of stability, phase relationships, and the role of epidote in magmatic evolution. Am Mineral 81: 424-474.

SHCHERBAKOV VD, PLECHOV PY, IZBEKOV PE & SHIPMAN JS. 2011. Plagioclase zoning as an indicator of magma processes at Bezymianny Volcano, Kamchatka Contrib Mineral Petr 162: 83-99.

SHORE M & FOWLER AD. 1996. Oscillatory zning in minerals: a common phenomenon. Can Mineral 34: 1111-1126

SIAL AN. 1984. Litogeoquímica de elementos terras raras na caracterização de granitóides do espaço Cachoeirinha, Nordeste do Brasil. In: XXXIII Brazilian Congress of Geology, Annals. Rio de Janeiro: SBG, p. 2697-2702.

SIAL AN. 1990. Epidote-bearing calc-alkalic granitoids in Northeast Brazil. Rev Bras Geoc 20: 88-100.

SIAL AN. 1993. Contrasting metaluminous magmatic epidote-bearing granitic suites from two Precambrian Foldbelts in Northeast Brazil. An Acad Bras Cienc 65 (Supl. 1): 141-162.

SIAL AN & FERREIRA VP. 2000. Homogeneous $\delta^{18}O$ signature and the peritetic melting origin of Pedra Branca granodiorite pluton, state of Paraíba, NE Brazil.

SIAL AN & FERREIRA VP. 2015. Magma associations in Ediacaran granitoids of the Cachoeirinha–Salgueiro and Alto Pajeú terranes, northeastern Brazil: Forty years of studies. J S Am Earth Sci: 113-133.

SIAL AN, FERREIRA VP, FALLICK AE & CRUZ MJM. 1998. Amphibole-rich clots in calc-alkalic granitoids in the Borborema Province, northeastern Brazil. J S Am Earth Sci 11: 457-472.

SIAL AN, TOSELLI AJ, SAAVEDRA J & FERREIRA VP. 1999. Emplacement, petrological and magnetic susceptibility characteristics of diverse magmatic epidote bearing granitoids in Brazil, Argentina and Chile. Lithos 46: 367-392.

SIAL AN, VASCONCELOS PM, FERREIRA VP, PESSOA RR, BRASILINO RG & MORAIS NETO JM. 2008. Geochronological and mineralogical constraints on depth of emplacement and ascension rates of epidote-bearing magmas from northeastern Brazil. Lithos 105: 225-238.

SILVA FILHO AF, GUIMARÃES IP & THOMPSON RN. 1993. Shoshonitic and ultrapotassic Proterozoic intrusive suites in the Cachoeirinha–Salgueiro Belt, NE Brazil: a transition from collisional to post-collisional magmatism. Precambrian Res 62: 323-342.

SIQUEIRA R, SIAL AN & FERREIRA VP. 2018. Granitos com epidoto magmático e clinopiroxênio: plutons Tamboril e Olho d'Água, Terreno Cachoeirinha–Salgueiro, Nordeste do Brasil. Geochim Bras 12: 20-39.

SISSON TW, RATAJESKI K, HANKINS WB & GLAZNER AF. 2005. Voluminous granitic magmas from common basaltic sources. Contrib Mineral Petr 148(6): 635-661.

TAKAHASHI M, ARAMAKI S & ISHIHARA S. 1980. Magnetite series ilmenite series vs I–type S–type granitoids. Min Geol Special Issue 8: 13-28.

TINDLE AG & WEBB PC. 1990. Estimation of lithium contents in trioctahedral micas using microprobe data: application to micas from granitic rocks. Eur J Mineral: 595-610.

TINDLE AG & WEBB PC. 1994. PROBE-AMPH—a spreadsheet program to classify microprobe-derived amphibole analyses. Comput Geosci 20(7-8): 1201-1228.

TROPPER P, MANNING CE & ESSENE EJ. 2002. The substitution of Al and F in titanite at high pressure and temperature: experimental constraints on phase relations and solid solution properties. J Petrol 43: 1787-1814.

THOMPSON AB & ELLIS DJ. 1994. $CaO+MgO+Al_2O_3+SiO_2+H_2O$ to 35 kb; amphibole, talc, and zoisite dehydration and melting reactions in the silica-excess part of the system and their possible significance in subduction zones, amphibolite melting, and magma fractionation. Am J Sci 294(10): 1229-1289.

TULLOCH A. 1979. Secondary Ca-Al silicates as low-grade alteration products of granitoid biotite. Contrib Mineral Petr 69: 105-117.

VAN SCHMUS WR, KOZUCH M & BRITO NEVES BB. 2011. Precambrian history of the Zona Transversal of the Borborema Province, NE Brazil: insights from Sm-Nd and U-Pb geochronology. J S Am Earth Sci 31(2-3): 227-252.

WATSON EB. 1987. The whole of accessory minerals in granitoids geochemistry. In: Hutton Conference of the Origin of Granites 4: 209-211.

WATSON EB & HARRISON MT. 1983. Zircon saturation revisited: temperatures and composition effects in a variety of crustal magma types. Earth Planet Sc Lett 104: 381-397.

WONES DR. 1989. Significance of the assemblage titanite+magnetite+quartz in granitic rocks. Am Mineral 74: 744-749.

ZEN EA. 1988. Tectonic significance of high pressure plutonic rocks in the Western Cordillera of North America. In: Ernst WG (Ed), Metamorphism and Crustal Evolution of the Western United States, Rube, vol. VIII. Prentice-Hall, Engelwood Cliffs, New Jersey, p. 41-71.

SUPPLEMENTARY MATERIAL

Table SI. Microprobe analyses of plagioclase from Tamboril (TAM) and Olho d'Água (OA) plutons.

Table SII. Microprobe analyses of amphibole from Tamboril (TAM) and Olho d'Água (OA) plutons. Tindle and Webb (1994) methods calculated to Fe partition (Fe2+ – Fe3+) and H2O contents.

Table SIII. Microprobe analyses of biotite from Tamboril (TAM) and Olho d'Água (OA) plutons. Tindle & Webb (1990) approach was used to calculate Li2O and H2O contents.

Table SIV. Microprobe analyses of epidote from Tamboril (TAM) and Olho d'Água (OA) plutons.

Table SV. Microprobe analyses of titanite from the Tamboril (TAM) and Olho d'Água (OA) plutons.

Table SVI. Microprobe analyses of clinopyroxene from Tamboril (TAM) and Olho d'Água (OA) plutons.

How to cite

SIQUEIRA R, SIAL AN & FERREIRA VP. 2021. Crystallization conditions of two adjacent epidote + diopside-bearing granitic stocks, northeastern Brazil. An Acad Bras Cienc 93: e20210535. DOI 10.1590/0001-3765202120210535.

Manuscript received on April 9, 2021;
accepted for publication on July 9, 2021

RENAN SIQUEIRA
https://orcid.org/0000-0003-3033-3634

ALCIDES N. SIAL
https://orcid.org/0000-0001-7584-0600

VALDEREZ P. FERREIRA
https://orcid.org/0000-0003-3220-7113

Federal University of Pernambuco, Department of Geology, NEG–LABISE, Av. Acadêmico Hélio Ramos, s/n, Cidade Universitária, 50740-530 Recife, PE, Brazil

Correspondence to: **Renan Siqueira**
E–mail: renan_siqueira3@hotmail.com

Author contributions

Renan Siqueira: Conceptualization, investigation, resources, visualization, methodology, formal analysis, writing and editing. Alcides N. Sial: Formal analysis, investigation, writing – review & editing, funding acquisition. Valderez P. Ferreira: Formal analysis, investigation, writing – review & editing.